NATIONAL RADIO ASTRONOMY OBSERVATORY
Green Bank, West Virginia

Electronics Division Internal Report No. 12

THE CHARACTERISTICS OF THE 85-FOOT TELESCOPE AT 21 CM WAVELENGTH WITH A HORN-FEED AND A COMPOUND DIPOLE FEED

By Peter G. Mezger

July 1963

Rerun 11/10/66: 50 Copies

THE CHARACTERISTICS OF THE 85-FOOT TELESCOPE AT 21 CM WAVELENGTH WITH A HORN-FEED AND A COMPOUND DIPOLE FEED

1. Introduction

Because of the more heavily tapered primary pattern of horn-feeds, telescopes which are designed for use with horn-feeds have greater focal distance and consequently flatter parabolic reflectors than have telescopes with dipole feeds. Now, the smaller the aperture angle of the telescope, the stronger is the spillover effect. To reduce spillover effect heavily tapered horn-feeds are used, which result in a loss of gain and angular resolution of the telescope. To avoid these difficulties the Jasik Laboratories have designed a compound dipole feed for the NRAO 85-foot telescope, which gives a nearly constant illumination of the paraboloid reflector and drops abruptly more than 20 db at the edge of the dish. The characteristics of the 85-foot telescope in conjunction with the Jasik feed have been measured at the frequencies 1385, 1405, and 1425 Mc. To compare this feed with the horn-feed, which has been used hitherto at the 85-foot telescope, the characteristics of the telescope were also measured with the horn-feed.

Below are the definitions of terms used in the described antenna calibration:

(1) Antenna temperature -- will refer to the output-connector of the antenna feed.

(2) Main beam -- $f_m = \exp\left\{-\zeta^2/(0.6\widetilde{\omega})_E^2 - \eta^2/(0.6\widetilde{\omega})_H^2\right\}$ is the gaussian approximation of the main beam. $\widetilde{\omega}_E$ and $\widetilde{\omega}_H$ are the half-power widths in the electrical (E) and the magnetic (H) plane of the antenna.

(3) Main beam solid angle -- $\Omega_m = \int\int_{-\infty}^{+\infty} d\zeta d\eta f_m(\zeta,\eta) = 1.133\ \widetilde{\omega}_E\ \widetilde{\omega}_H$ as compared to the antenna solid angle $\Omega = \int_{\text{sphere}} f d\Omega$.

(4) Radiation efficiency -- $\eta = \dfrac{\text{available power at the feed connector}}{\text{total power absorbed by the antenna}}$

(5) Main beam stray factor -- $\beta_m = 1 - \Omega_m/\Omega$

(6) Directivity -- $D = 4\pi/\Omega$. The gain G of the antenna is related to the directivity by $G = \eta D$. The main beam directivity $D_m = 4\pi/\Omega_m$. Between D and D_m the relation $D = (1 - \beta)D_m$ holds.

All other antenna terms used and relations between those terms are well known from antenna theory.

For the gain calibration of the antenna the flux densities of Cas A and Cyg A have been used. For Cas A the flux density

$$S_{1440}(\text{Cas A}) = 247.10^{-25} \text{ W/m}^2\text{Hz} \tag{7}$$

and a spectral law $S \sim \nu^{-0.8}$; for the flux of Cyg A the relation

$$\frac{S(\text{Cas A})}{S(\text{Cyg A})} = 1.57 \tag{8}$$

has been assumed.

For the determination of the different stray factors of the antenna, the thermal radiation of the atmosphere and of the earth's surface has been used. The radiation temperature of the atmosphere is related to the atmospheric attenuation by

$$T_{at} = \overline{T}_{air}(1 - p^{F(z)}) \tag{9}$$

where p = the transmission coefficient of the atmosphere at zenith, $z = 90°-h$ (h = elevation angle and F(z) = the air-mass (Bemporad) function). $\overline{T}_{air}$ is a mean value of the air temperature within the line of sight and may be considered as independent of the elevation angle h. The radiation temperature of the earth's surface is ϵT_o, where T_o is the physical temperature and ϵ is the emission coefficient of the earth's surface. For wood covered regions $\epsilon \approx 1$ seems to be a realistic assumption.

2. Receiver and Temperature Calibration

Figure 1 shows the block-diagram of the receiver front end used in the antenna measurement. The principle of gain modulation technique is known, so no further discussion is needed. The relation between input noise temperature T and output voltage V at the first detector is not linear but follows the detector law $T = CV^{\alpha}$. Let T_t be the total noise temperature of the system, V_t the corresponding DC-voltage at the first detector, ΔT_c the calibration mark, and ΔV_c the corresponding change of the detector voltage output. Let the unknown antenna temperature T_A produce a voltage V_A. As long as $\Delta T_c \ll T_t$ the relation holds [1].

$$T_A = \frac{\Delta T_c}{\Delta V_c} V_A \mu (V_A/V_t) \tag{10}$$

The general relation is

$$T_A = \Delta T_c \frac{V_A \cdot \mu (V_A/V_t)}{\Delta V_c \cdot \mu (\Delta V_c/V_t)} \tag{11}$$

The correction factor μ applies for the nonlinearity of the detector law and may be found for various exponents α as a function of $\Delta V/V_t$ in ref. [1]. $\alpha = 1.63$ and V_t (detector current = 200 μA) = 322 mV have been checked experimentally for this particular receiver. The audio gain has been checked for each record.

The two calibration marks have been calibrated against a heated resistance [2] and against a load cooled in liquid nitrogen. One mark corresponds to a temperature difference of about 20 °K, and the other of about 200 °K.

3. Adjustment of the Antenna Feed

The antenna feed has been adjusted by maximizing the antenna temperatures of different radio sources. A theoretical analysis shows that the antenna gain is hardly affected by a slight radial defocusing (but a deviation between mechanical and electrical antenna axes results). For the gain variation as a function of the axial distance Δf_{ax} between the phase center of the feed and the focal point of the paraboloid reflector, an expression has been derived

$$\frac{G}{G_o} = \left[\frac{\sin \frac{u}{2}}{\frac{u}{2}}\right]^2 \tag{12}$$

where G_o is the maximum gain, $u/2 = \pi (1 - \cos \frac{\psi}{2}) \Delta f_{ax}/\lambda$ and $\psi = 120°$ is the aperture angle of the 85-foot antenna. Function (12) is plotted for $\lambda = 21$ cm in Figure 2. The measured normalized antenna temperatures of Cas A and Cyg A, respectively, obtained with the Jasik feed ($\odot$) and with the horn-feed (+) for various distances of their phase center referred to the mechanical focal point of the parabolic reflector, are also shown in Figure 2. The final positions of the feeds for maximum antenna temperature (and consequently, as we hope, maximum gain) are shown in Figures 3a through 3c.

The designed focal length of the telescope is 10.963 m. The location of the phase center of the horn-feed is assumed to lay $\lambda/8$ inside the horn, measured from the aperture plane. This leads from Figure 3b to a distance of $d_1 - \lambda/8 = 11.008$ m for the electrically determined focal length. The location of the phase center of the Jasik feed is assumed to be at a distance $\lambda/12$ in front of the reflector plate; this leads to a focal length $d_2 + \lambda/12 = 11.021$ m. Whereas the two electrically obtained focal lengths are well consistent, the difference between designed and electrically measured focal lengths of 4 and 6 cm, respectively, are too big to be explained by the uncertainty of the electrical focusing, as may be seen from Figure 2.

4. Model of the Antenna Pattern

It is experimentally impossible to measure the sidelobes of large antennas below a certain attenuation; this limit lies generally between 50 and 60 db. It is, however, possible to measure integrated values of the antenna pattern, as will be shown. To derive the antenna characteristics from such integrated values, a certain model of the antenna pattern has to be assumed.

The simplest model consists of a main beam pattern conforming to equation (2) and a stray region with a constant attenuation, which may be described by the main beam stray factor, equation (5). This model is reasonable for measurements of radio sources whose angular diameter is smaller than the beamwidth of the antenna.

If the brightness temperatures of radio sources are to be measured, whose diameters are considerably greater than the antenna beamwidth, or if absolute antenna temperatures are to be measured, it must be considered that the attenuation of the first sidelobes is considerably less than the average attenuation of the remaining sidelobes. By using the radio radiation of the sun it may be shown that the sidelobes with a low attenuation occur only in a small range about the main axes of the antenna, which we will define as stray region I, and, perhaps, in the spillover direction of the antenna. In the remaining region -- defined as stray region II -- a constant mean attenuation is a fairly good approximation.

Figure 4 shows this antenna model, which will be used in the following discussion. The stray regions may be described either by their solid angles

$$(13) \qquad \Omega_I = \int_{\text{stray reg. I}} f\,d\Omega \qquad \Omega_{II} = \int_{\text{stray reg. II}} f\,d\Omega$$

with antenna solid angle $\Omega = \Omega_m + \Omega_I + \Omega_{II}$

or by their stray factors

$$(14) \qquad \beta_I = \Omega_I/\Omega \qquad \beta_{II} = \Omega_{II}/\Omega$$

with main beam stray factor $\beta_m = \beta_I + \beta_{II}$

In these definitions the spillover lobes are contained in the stray region II. If necessary the definitions may easily be expanded for a stray region III describing only the spillover effect.

5. The Measurements

The most important results of our measurements are compiled in table 1. The accuracy with which antenna temperatures between 10 and 300 °K can be measured has been estimated to be $\pm$ 3%; so $\pm$ 3% is also the accuracy of all antenna temperatures in table 1 with the exception of sky pole temperature, which has been measured as the difference between the temperature of the reference load and the antenna temperature in

TABLE 1

Measured Temperatures	Symbols	Jasik Feed			Horn 1425 Mhz
		1385 Mhz	1405 Mhz	1425 Mhz	
Antenna temperature Cas A	T_A (Cas A)	291 °K	255 °K	244 °K	257 °K
Antenna temperature Cyg A	T_A (Cyg A)	171 °K	162 °K	159 °K	164 °K
Sky pole temperature	T_{sp}	28 ± 9 °K	27 ± 9 °K	---	51 ± 9 °K (?)
(Corresponding outside temp.)	$T_{out\ s}$	---	16 °C	---	18 °C
Antenna temperature at an elevation angle h = 1° 30', a = 90°	T_{horiz}	---	223 °K (?)	253 °K	273 °K
(Corresponding outside temp.)	$T_{out\ s}$	---	288 °K	290 °K	290 °K
	$T_{out\ s} - T_{hor}$	---	57 °K (?)	37 °K	17 °K
First sidelobes	$\frac{T_A \text{ (Cas A)}}{T_A \text{ (sidelobe)}}$	---	15.9 & 13.9 db (magn. plane)		21.9 and > 26 db (45 between electric and magn. plane)
Half power beamwidth magnetic plane	$\textcircled{\sim}_H$	33.5' ± 0.2'	33.5' ± 0.2'	33.5' ± 0.2'	36!7
Half power beamwidth electric plane	$\textcircled{\sim}_E$	37' ± 0.2'	37' ± 0.2'	37.1' ± 0.2'	36!0

the sky pole. Consequently, the accuracy of 3% is valid for this difference temperature of about 300 °K.

The main beam pattern of the 85-foot antenna with the Jasik feed has been measured by means of drift curves (magnetic plane) and declination scans (electric plane). The measured points have been plotted in Figures 5a and 5b for the Jasik feed at 1425 Mc. The solid curves are the gaussian main beam approximations corresponding to equation (2) in which the beamwidths α_E and α_H of table 1 have been inserted.

The first sidelobes of the antenna have been measured only in the magnetic plane in the case of the Jasik feed. In the case of the horn, the beamwidth and the sidelobes have been measured in a plane exactly between magnetic and electric planes of the horn-feed.

In a so-called "elevation run" the antenna temperature as a function of the elevation angle h at the constant azimuth angle a = 90° (west) has been measured. The result is shown for both the horn-feed and the Jasik feed in Figure 6. In the same diagram also is plotted the brightness temperature of the sky and the horizon. The radiation temperature of the atmosphere has been calculated by means of equation (9) with $-\log p = 0.005_4$ [3] and $\overline{T}_{air} = 265$ °K. For the radiation temperature of the horizon, ϵT_o, the emission coefficient $\epsilon = 1$ and for T_o the "outside temperature" has been assumed. The antenna temperatures at zenith angle and below the horizon are of special interest. The value T_z may be obtained from the measured value of the sky pole (table 1) by subtracting 2 °K. The value $T_{horizon}$ in table 1 has been measured as the difference between the reference load temperature and the horizon temperature by using the 20 °K calibration.

Table 2 shows the result of three different calibrations of the calibration marks I and II at the beginning, in the middle and at the end of the measurements.

TABLE 2

Date	Frequency	Calibration Mark I	Calibration Mark II
6-26-63*	1385 Mc	220 °K	16.2 °K
7-1-63**	1425 Mc	217 °K	18.9 °K
7-8-63	1425 Mc	211 °K	14.5 °K

* Between calibrations on 6-26 and 7-1 the cable between feed and receiver input changed.
** The cable used on the load in this calibration was 40 cm long, whereas the cables used in the other two calibrations were 25 cm long.

TABLE 3

Quantity	Symbols	Jasik Feed			Horn 1425 Mhz
		1385 Mhz	1405 Mhz	1425 Mhz	
Effective area of the antenna	A (Cas A)	314 m^2	279 m^2	271 m^2	285 m^2
	A (Cyg A)	290 m^2	278 m^2	277 m^2	285 m^2
Adopted mean value	A	302 m^2	278.5 m^2	274 m^2	285 m^2
Antenna efficiency A/Ag (Ag = 525 m^2)	η_A	57.5%	53%	52%	54%
Antenna solid angle	Ω	0.51 □	0.535 □	0.53 □	0.51 □
Main beam solid angle 1.133 θ_E θ_H	Ω_m	0.39 □	0.39 □	0.39 □	0.42 □
Stray factor $1 - \Omega_m/\Omega$	β_m	0.23_5	0.27	0.26_5	0.18
Radiation efficiency (estimated values)	η	0.98	0.98	0.98	0.99
Stray factor region II (calculated from sky pole temperature)	β_{II}		0.115		0.30 (?)
Main beam stray factor (calculated from horizon temperature)	β_m			0.26	0.14
Stray factor region I $\beta_m - \beta_{II}$	β_I		0.15_5		-0.14(?)

6. The Evaluation of the Measurements

Starting from the measured values which are compiled in table 1, we have calculated the characteristics of the 85-foot antenna. The results are compiled in table 3. We shall now explain these calculations.

Let f be a frequency slightly different from the frequency 1440 Mc, for which the flux of Cas A is known. Then the flux at this frequency f may be calculated from

$$(15) \qquad S_f = \frac{S_{1440}}{1 - 0.8\,\frac{\Delta f}{1440}} \qquad \text{where } \Delta_f = f - 1440$$

With equations (7) and (8) we get

TABEL 4

Frequency f	Flux Cas A	Flux Cyg A
1385 Mc	$255 \cdot 10^{-25}$ W/m²Hz	$162._5 \cdot 10^{-25}$ W/m²Hz
1405 Mc	$252 \cdot 10^{-25}$ W/m²Hz	$160._5 \cdot 10^{-25}$ W/m²Hz
1425 Mc	$249 \cdot 10^{-25}$ W/m²Hz	$158._5 \cdot 10^{-25}$ W/m²Hz

The efficient antenna area A can then be calculated from the relation

$$(16) \qquad S = \frac{2k\,T_A}{A} \qquad k = 1.38 \cdot 10^{-23}\ \text{Ws/°K}$$

If A is known, the antenna solid angle Ω can be calculated from the relation

$$(17) \qquad \Omega = \frac{41\,253}{4\pi}\,\frac{\lambda^2}{A} \qquad \lambda = \frac{c}{f}\ \text{wavelength}$$

The main beam solid angle can be calculated by using equation (3) and the measured half-power beamwidth. From Ω_m and Ω the main beam stray factor can be derived, using equation (5).

There is no possibility of measuring the radiation efficiency η ; so this value has been estimated.

With the antenna pointed to zenith we have obtained the antenna temperatures $T_z = T_{sp} - 2\ ^\circ K$, where the values T_{sp} can be taken from table 1. By using the antenna pattern model shown in Figure 4 we can relate this measured antenna temperature to the radiation temperatures of the sky and the earth's surface.

$$(18) \qquad T_z = \eta \left[(1 - \beta_m + \beta_I)\, T_{at}(h = 90^\circ) + \frac{\beta_{II}}{2} \overline{T}_{sky} + \frac{\beta_{II}}{2} T_o \right] + (1 - \eta) T_o$$

With $\beta_m = \beta_I + \beta_{II}$ we obtain

$$(19) \qquad \beta_{II} = \frac{\frac{1}{\eta}\left[T_z - (1 - \eta)\, T_o\right] - T_{at}(h = 90^\circ)}{\frac{1}{2}\left[\overline{T}_{sky} + T_o\right] - T_{at}(h = 90^\circ)}$$

With $\overline{T}_{sky} = 10\ ^\circ K$, $T_{at}(h = 90^\circ) = 2.5\ ^\circ K$ and $T_o = 290\ ^\circ K$ and the measured antenna temperatures we found the values β_{II} indicated in table 3. Since the accuracy of the measured sky pole temperature is relatively low and since for the horn-feed this result is not consistent with the other results, we have put a (?) to the values of β_I and β_{II} for the horn-feed.

For the antenna temperature, which has been measured, when the antenna was pointed below the horizon a similar expression to equation (18) can be derived. Figure 7 shows the skyline and the position of the antenna, corresponding to this measurement. $\overline{T}_{sky}(I)$ means the sky temperature averaged over the stray region I; $\overline{T}_{sky}(II)$ is the corresponding mean value for the stray region II. Then

$$(20) \qquad T_{horiz} = \eta \left[(1 - \beta_m)\, T_o + \frac{\beta_m}{2} T_o + \frac{\beta_I}{2} \overline{T}_{sky}(I) + \frac{\beta_{II}}{2} \overline{T}_{sky}(II) \right] + (1 - \eta)\, T_o$$

from which we obtain

$$(21) \qquad \beta_m = 2\, \frac{T_o - \frac{1}{\eta}\left[T_{horiz} - (1 - \eta)\, T_o\right] - \frac{\beta_{II}}{2}\left[\overline{T}_{sky}(I) - \overline{T}_{sky}(II)\right]}{T_o - \overline{T}_{sky}(I)}$$

With $\overline{T}_{sky}(I) = 30\ ^\circ K$ and $\overline{T}_{sky}(II) = 7\ ^\circ K$ we have obtained values for β_m which agree very well with the corresponding values obtained from the relation $\beta_m = 1 - \Omega_m / \Omega$, at least in the case of the Jasik feed.

7. Discussion of the Results

The accuracy of each individual measurement is not very high. But since we have two independent measurements to determine the main beam stray factor, it is possible to check the most important results and we think that it may be possible to obtain useful models of the secondary pattern of the 85-foot telescope with the Jasik feed and the horn-feed.

Table 3 shows that the antenna efficiency and consequently the antenna gain for both feeds is approximately the same, while the beamwidth and therefore the main beam solid angle of the antenna with the Jasik feed is considerably smaller. Since between the antenna gain G and the main beam solid angle the relation holds

$$G = \eta_R (1 - \beta_m) \frac{4\pi}{\Omega_m} \tag{22}$$

these two results are only consistent if the increase of the factor $\eta_R (1 - \beta_m)$ in the case of the Jasik feed just compensates the higher main beam directivity $D_m = 4\pi/\Omega_m$. The two independent measurements of the main beam stray factor β_m shows that this is true indeed.

The measurement of the zenith temperature and consequently the determination of the stray factor β_{II} are by far the most inaccurate. It is therefore obvious that the stray factor $\beta_{II} = 0.30$ in the case of the horn-feed must be wrong, since always $\beta_{II} \leq \beta_m$. Probably the most reasonable assumption is that in this case $\beta_{II} = \beta_m = 0.16$ (the mean value of the two independent measurements). This means that the sidelobe attenuation of the antenna pattern in the stray region II with the horn-feed is so high that the contribution of this region to the total stray factor is negligible. In this case the main beam stray factor is essentially caused by the spillover effect. On the other hand, the stray factor β_{II} of the antenna with the Jasik feed is relatively low and consequently the spillover effect seems to be considerably smaller. But the attenuation of the sidelobes, as may also be seen from the direct measurements of the attenuation of the first sidelobes in table 1, is very low in the stray region and consequently the contribution of this region to the total stray factor is so strong that the main beam stray factor of the antenna with the Jasik feed is even greater than with the horn-feed.

From calculations, which are based on the measured primary pattern of the Jasik feed, an antenna efficiency between 70 and 80% is expected, whereas the measured efficiency lays between 50 and 60%. It could be argued, however, that the losses in the Jasik feed are higher (lower radiation efficiency) than we have estimated. To account for the discrepancy between measured and expected efficiency, the radiation efficiency η should be 0.75 instead of the estimated value 0.98. It is now easy to give an upper limit for the feed losses assuming that no spillover and no diffraction lobes in the backward direction of the feed exist. Then the term $\beta_{II}/2 \cdot T_o$ in equation (18) vanishes and the relation

$$(1 - \eta) = \frac{T_z - 3\ ^\circ K}{T_o} \tag{23}$$

holds, where 3 °K stands for the term in brackets. With the values $T_z = 25$ °K and $T_o = 300$ °K we find $\eta = 0.93$ as a lower limit for the radiation efficiency of the Jasik feed.

These results lead to the following conclusions:

1. The antenna efficiency for the Jasik feed remains approximately the same ($\approx$ 54%) as for the normally used horn-feed.

2. The spillover is considerably reduced by the Jasik feed at the expense of a much higher near sidelobe level.

For radioastronomical observations this is not a real improvement of the antenna because of source confusion and antenna smoothing problems.

It is not within the scope of this report to explain why it was impossible to reduce the spillover and to improve the antenna efficiency simultaneously. It would, however, be of interest to know whether this is a general rule or an inherent property of this special feed design.

It is also worth noticing that the feed pattern of the Jasik feed shows a very high rotational symmetry, whereas the secondary pattern is assymmetrical with the narrower beam in the magnetic plane. This could be caused by the four feed support legs of the 85-foot telescope because of the larger dimensions of the Jasik feed.

Acknowledgment

The author wishes to express his appreciation to the technicians and telescope operators for their assistance.

Literature

[1] Hvatum, H.: Detector Law. Electronics Division Internal Report No. 6 (December 1962).

[2] Ross, Dewey: Thermal Calibration of a Radiometer. Electronics Division Internal Report No. 4 (October 1962).

[3] Altenhoff, W. and Mezger, P. G.: Radioastronomische Messungen bei der Frequenz 1370 MH_Z zur Erprobung eines parametrischen Vorverstaerkers. Z. f. Astrophysik 57, pp. 172-182 (1963).

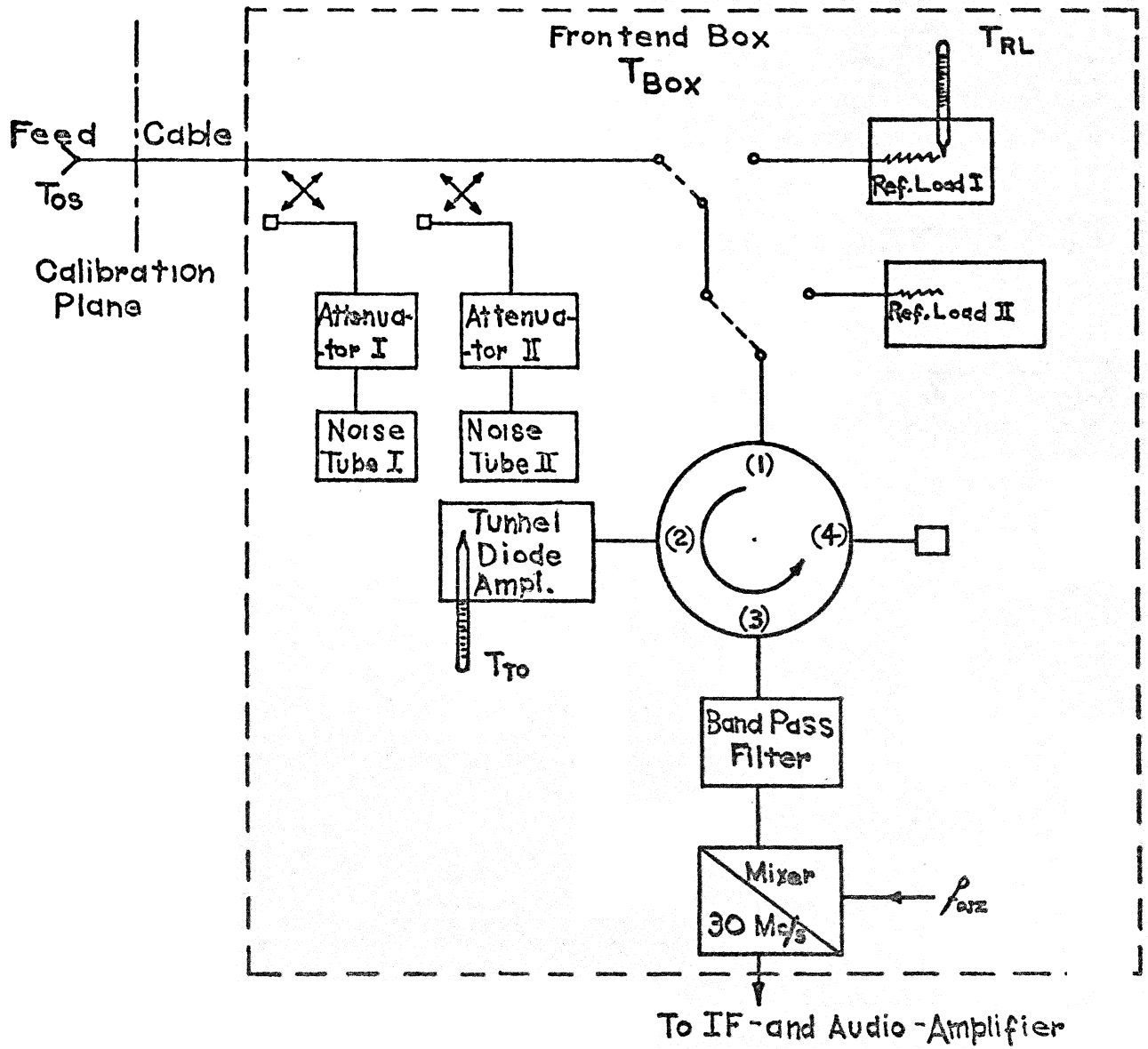

Fig. 1 Block diagram of HF-part and calibration system of the gain-modulated receiver used for the antenna measurements

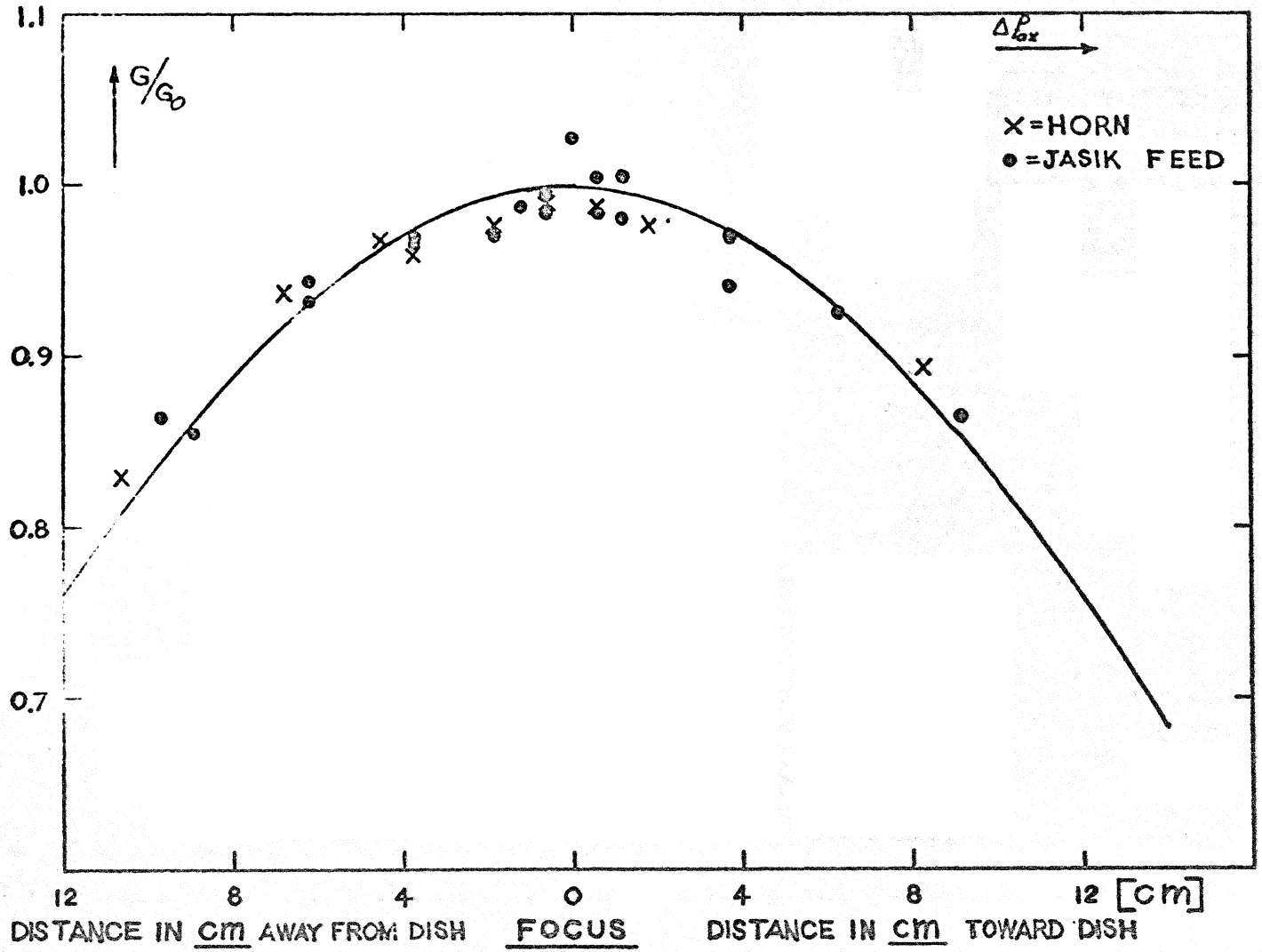

Fig. 2 Theoretical and measured variation of the gain of the 85-foot telescope as a function of the axial defocusing of the feed

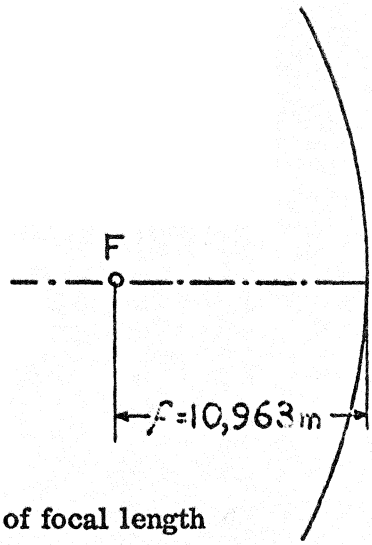

Fig. 3 a Definition of focal length

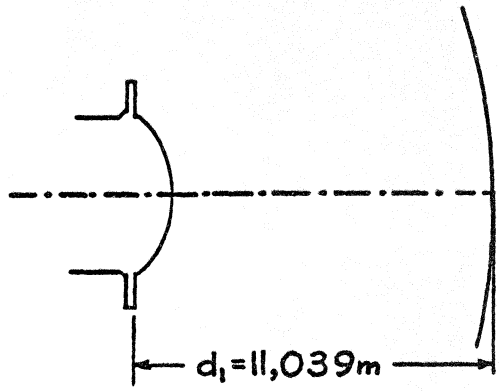

Fig. 3 b Definition of distance d_1 in the Jasik feed adjustment

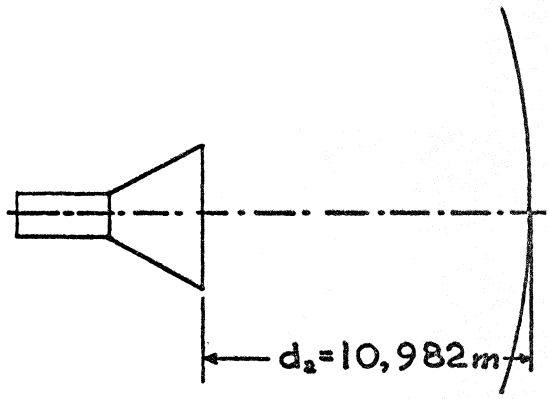

Fig 3 c Definition of distance d_2 in the horn adjustment

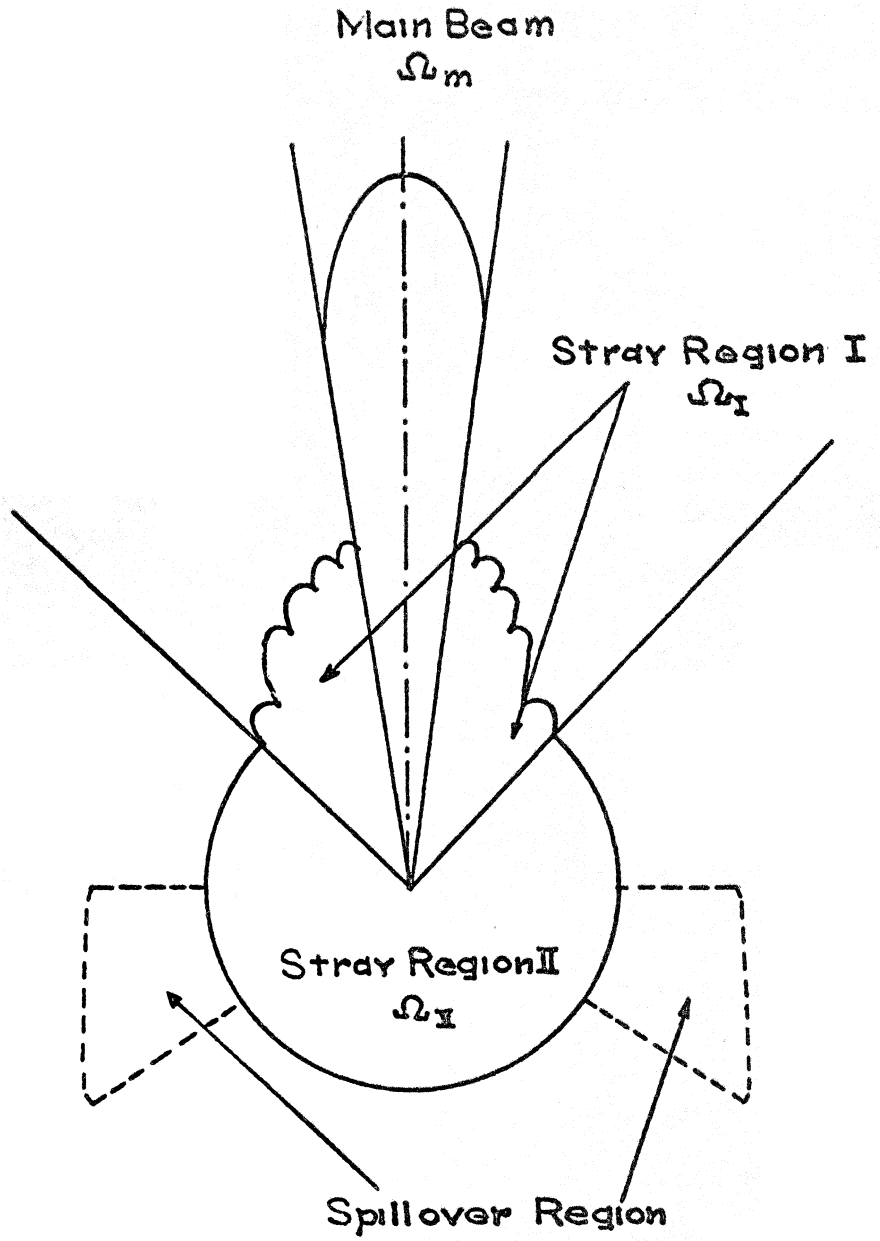

Fig. 4 Model of the antenna pattern, satisfactory for most radioastronomical measurements. Rotation symmetry with respect to the antenna main axes is assumed.

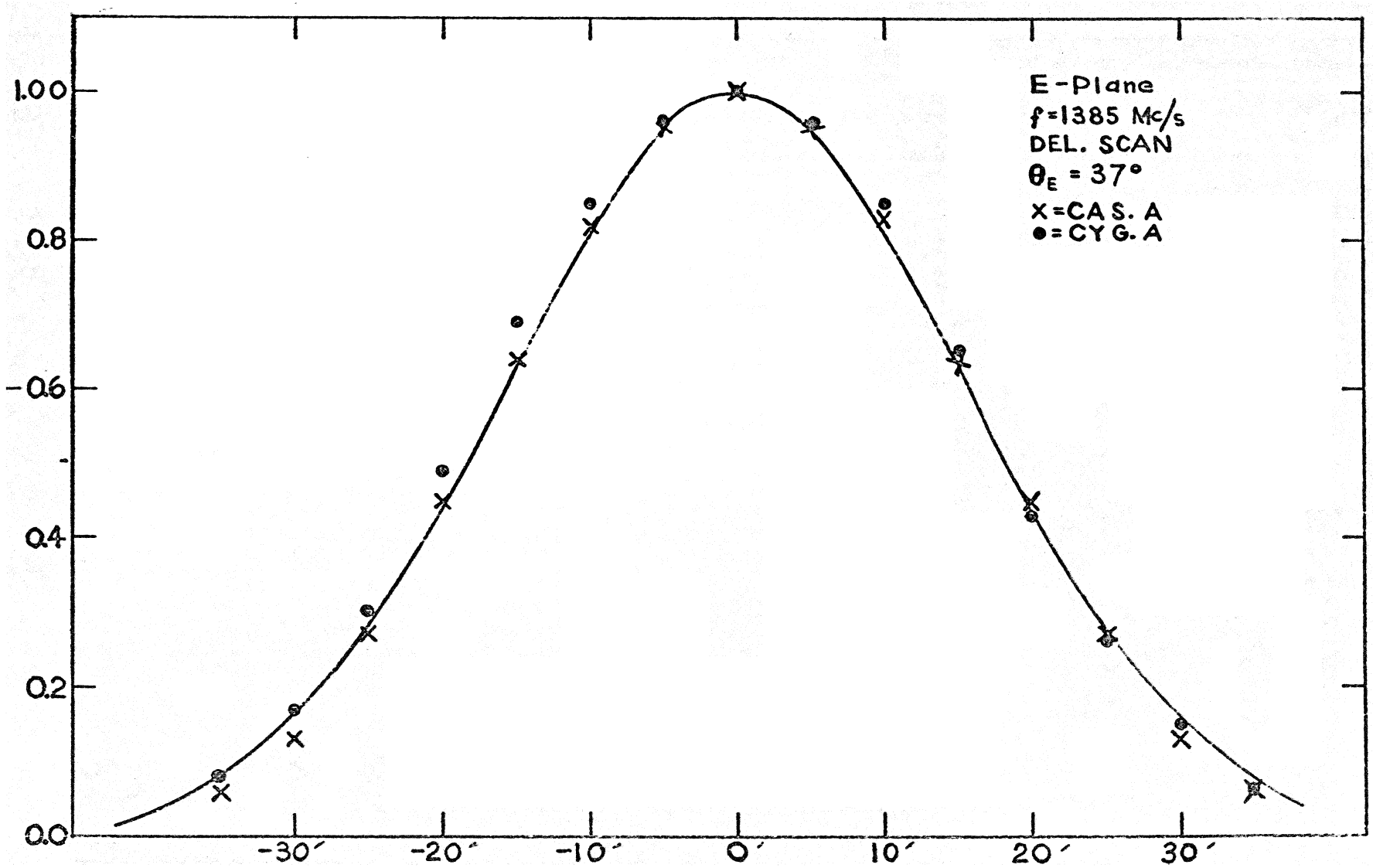

Fig. 5a Measured main beam pattern in the E-plane of the Jasik feed at 1385 Mc and Gauβ-approximation

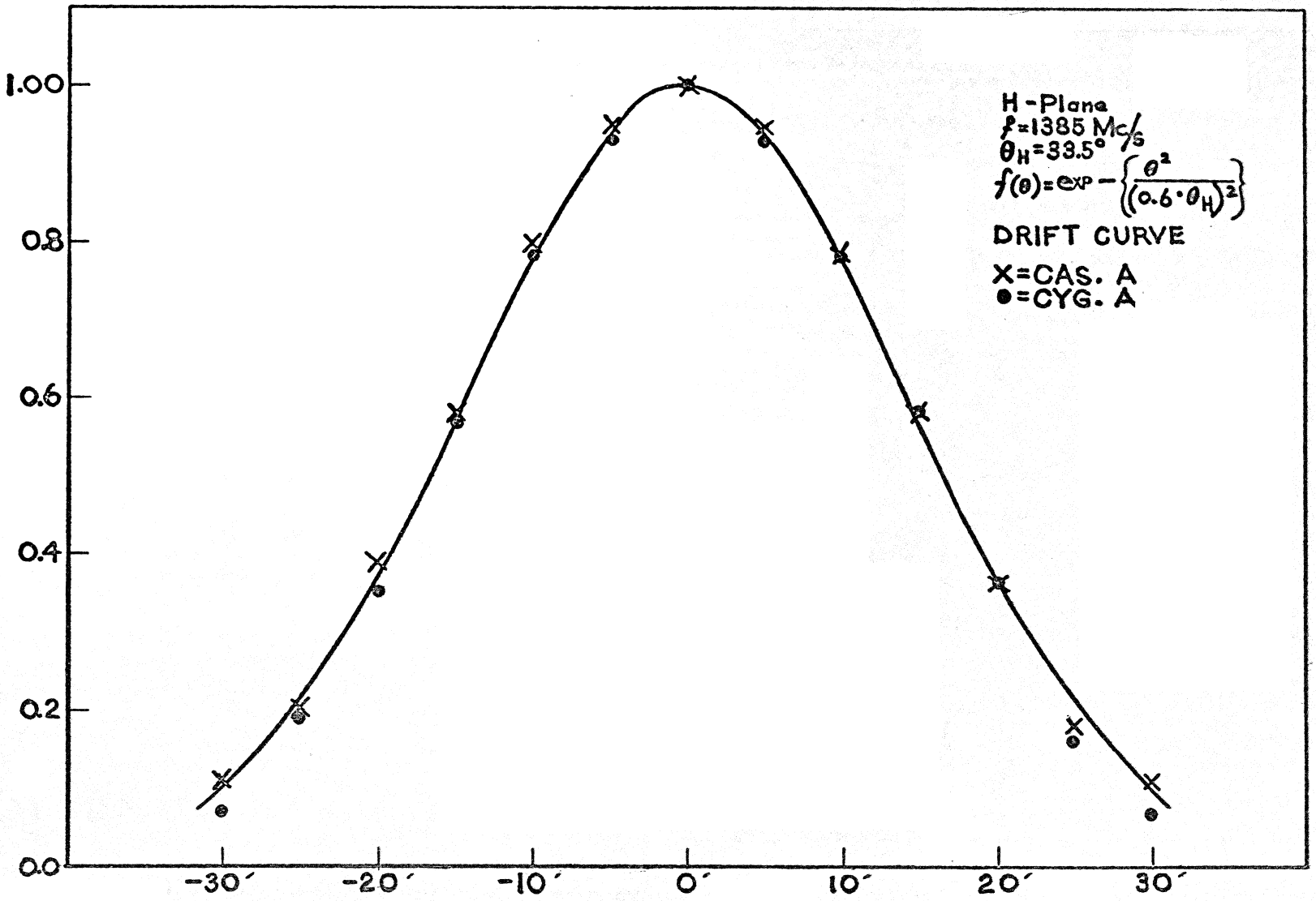

Fig. 5b Measured main beam pattern in the H-plane of the Jasik feed at 1385 Mc and Gauβ-approximation

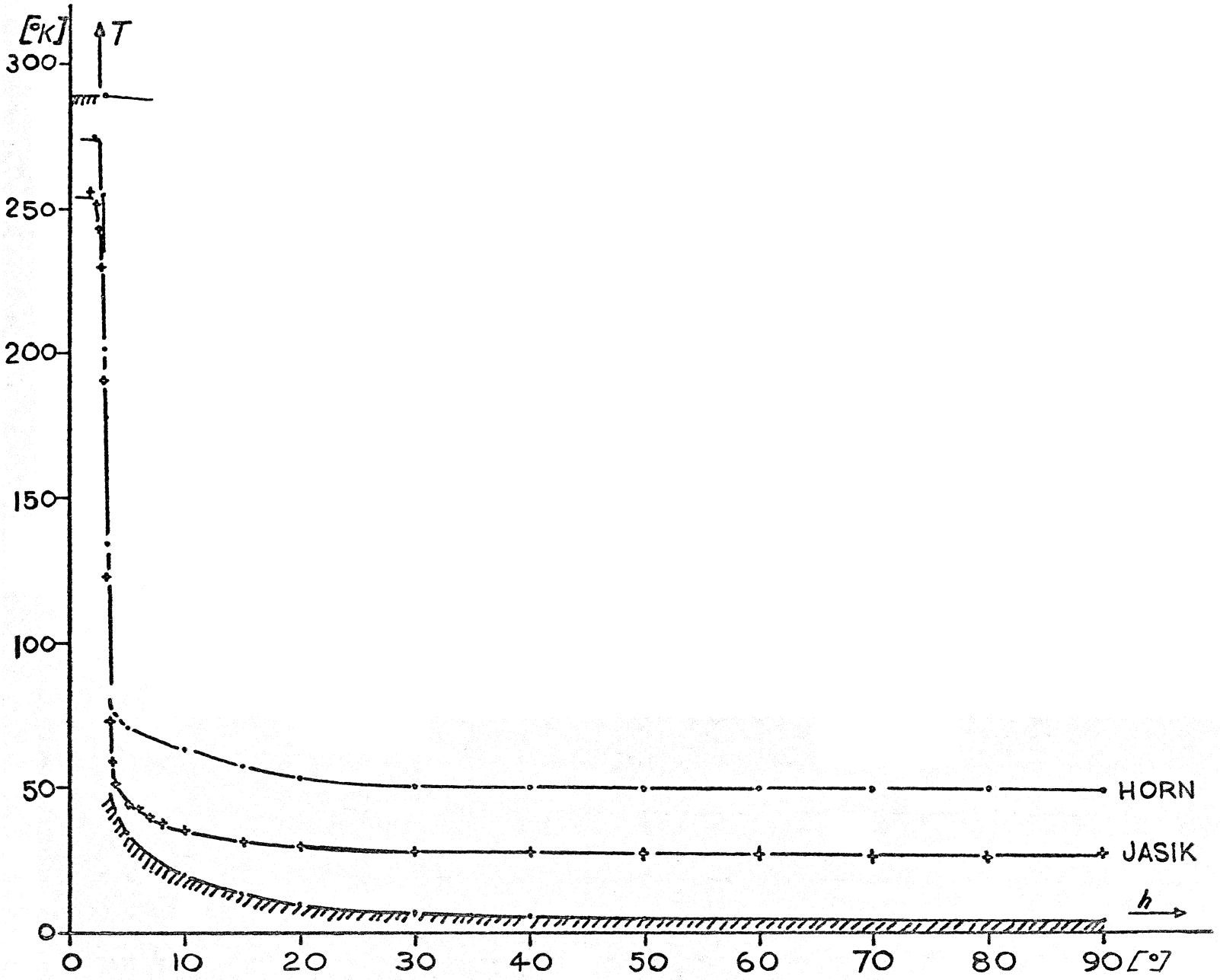

Fig. 6 Brightness temperature and with the 85-foot telescope measured antenna temperature as a function of the elevation angle h. at an azimuth angle a = const = 90° (west)

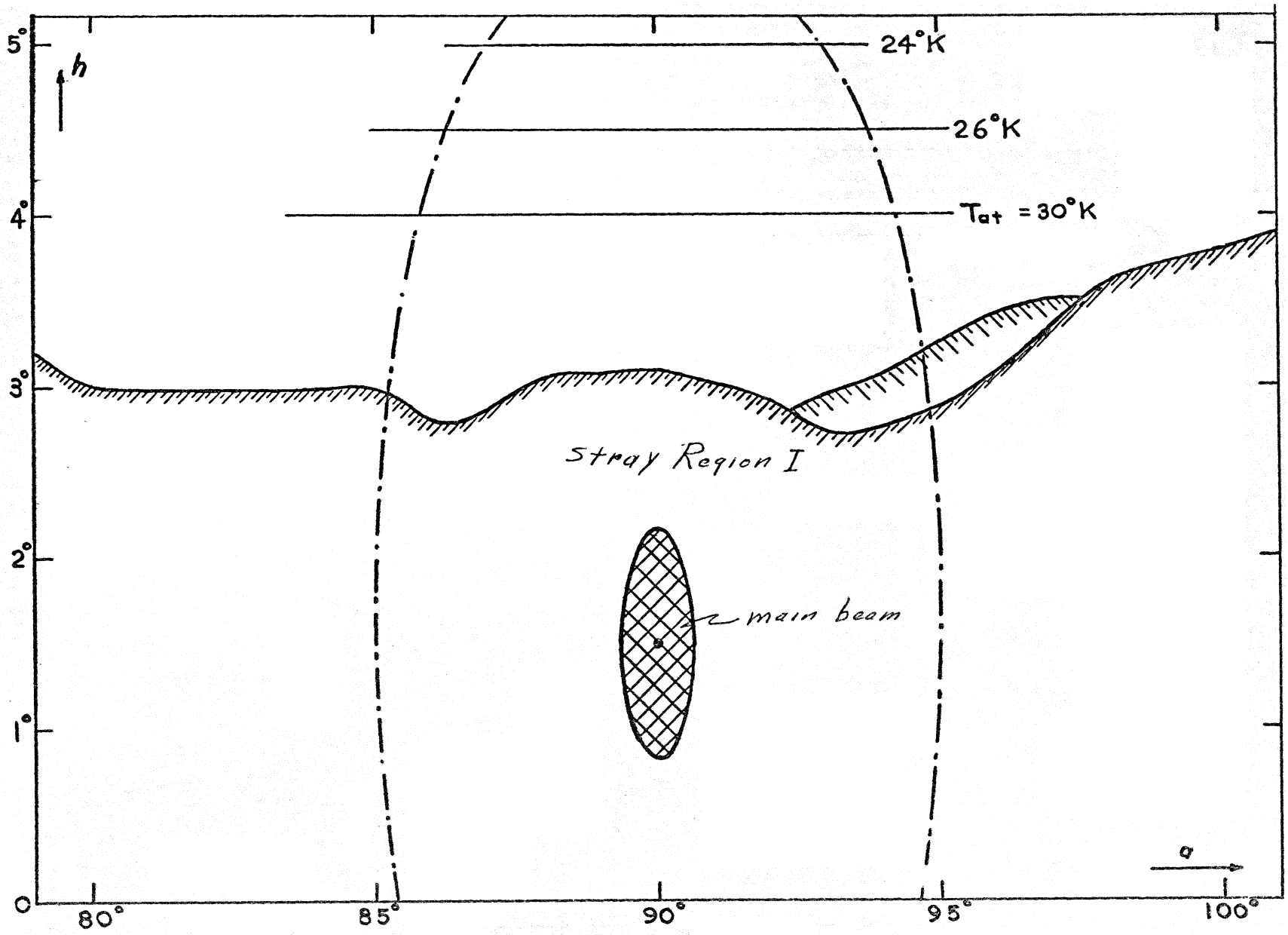

Fig. 7 Position of the antenna - especially of the main beam and the stray region I relative to the optical horizon at the elevation angle h = 1° 30', at which the horizon temperature has been measured